

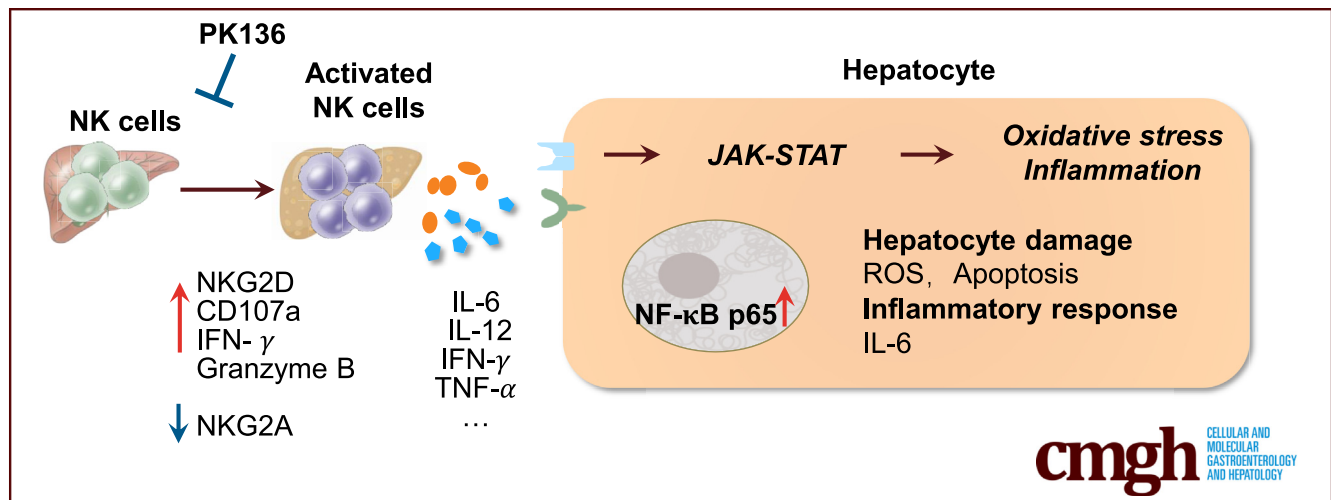
ORIGINAL RESEARCH

Activated Natural Killer Cell Promotes Nonalcoholic Steatohepatitis Through Mediating JAK/STAT Pathway



Feixue Wang,¹ Xiang Zhang,¹ Weixin Liu,¹ Yunfei Zhou,¹ Wenchao Wei,¹ Dabin Liu,¹ Chi Chun Wong,¹ Joseph J. Y. Sung,^{1,2} and Jun Yu¹

¹Institute of Digestive Disease and Department of Medicine and Therapeutics, State Key Laboratory of Digestive Disease, Li Ka Shing Institute of Health Sciences, CUHK Shenzhen Research Institute, The Chinese University of Hong Kong, Hong Kong SAR, China; and ²Lee Kong Chian School of Medicine, Nanyang Technology University, Singapore



SUMMARY

NK cells were activated in the evolution of experimental nonalcoholic steatohepatitis (NASH) and contributed to NASH pathogenesis via cytokine-JAK-STAT axis. Moreover, both NK cell deficiency *Nfil3*^{-/-} mice and PK136 dependent NK cell neutralization can significantly ameliorate NASH development.

BACKGROUND & AIMS: Hepatic immune microenvironment plays a pivotal role in the development of nonalcoholic steatohepatitis (NASH). However, the role of natural killer (NK) cells, accounting for 10%–20% of liver lymphocytes, in NASH is still unclear. In this study, we aim to investigate the functional significance of NK cells in NASH evolution.

METHODS: NASH was induced in mice fed methionine- and choline-deficient diet (MCD), choline-deficient high-fat diet (CD-HFD), or high-fat diet with streptozotocin injection (STAM model). NK cell deficient mice (*Nfil3*^{-/-}) and neutralization antibody (PK136) were used in this study.

RESULTS: Activated liver NK cells were identified with increased expression of NKG2D, CD107a, and interferon- γ but decreased inhibitory NKG2A. With NK cell deficiency *Nfil3*^{-/-} mice, the absence of NK cells ameliorated both MCD- and CDHF-induced NASH development with significantly decreased

hepatic triglycerides, peroxides, alanine aminotransferase, and aspartate aminotransferase compared with *Nfil3*^{+/+} mice. Further molecular analysis unveiled suppressed pro-inflammatory cytokines and associated signaling. Mechanistically, NK cells isolated from NASH liver secreted higher levels of pro-inflammatory cytokines (interferon- γ , interleukin 1 β , interleukin 12, CCL4, CCL5, and granulocyte-macrophage colony-stimulating factor), which could activate hepatic JAK-STAT1/3 and nuclear factor kappa B signaling and induce hepatocyte damage evidenced by elevated reactive oxygen species and apoptosis rate. Moreover, neutralization antibody PK136-dependent NK cell depletion can significantly alleviate MCD-induced steatohepatitis with suppressed cytokine levels and JAK-STAT1/3 activity.

CONCLUSIONS: NK cells in NASH liver are activated with a more pro-inflammatory cytokine milieu and promote NASH development via cytokine-JAK-STAT1/3 axis. Modulation of NK cells provides a potential therapeutic strategy for NASH. (*Cell Mol Gastroenterol Hepatol* 2022;13:257–274; <https://doi.org/10.1016/j.jcmgh.2021.08.019>)

Keywords: Nonalcoholic Steatohepatitis; Natural Killer Cell; Cytokine; JAK/STAT.

Nonalcoholic fatty liver disease (NAFLD), a spectrum of liver disease ranging from simple steatosis to steatohepatitis, is a major world health problem considering

its large contribution to liver-related morbidity.^{1,2} With the increasing burden of over-nutrition and obesity in the world, the global prevalence of this metabolic dysfunction associated liver disease keeps growing.^{3,4} Nonalcoholic steatohepatitis (NASH), characterized by steatosis, hepatocyte damage, and inflammation, is the advanced form of NAFLD that now represents one of the most common causes of cirrhosis and hepatocellular carcinoma (HCC).⁵ With growing body of evidence, it is now acknowledged that multiple factors including genetic modifier, environment, metabolism, and immune response are closely involved in the disease progression.^{6–9}

Lobular inflammation, one major histologic feature of NASH, along with abundant immune cell composition of liver, indicates that immune response is one of the key driving forces for disease progression. Previous investigations have identified that certain immune cells such as CD8⁺ T cell, macrophages, and invariant natural killer T cells (iNKT cells) contribute to NASH development.^{10,11} Natural killer cells (NK cells), harboring both direct cytotoxicity toward stressed or transformed cells as well as cytokine secretion potential, occupy 10% of total liver lymphocytes in mice and almost 50% in humans.^{12,13} The vital role of NK cells in liver homeostasis has been elucidated on multiple liver diseases including hepatic virus infection, fibrosis, and HCC. However, the role of NK cells in the evolution of NASH is still largely unclear. In this study, NK cells knockout mice (Nfil3^{-/-}) and NK cells neutralization antibody were used to study the effect of NK cells in NASH development. We identified that depletion of NK cells protected mice from NASH development. Mechanistically, NK cells promoted NASH progression through secreting multiple cytokines, which trigger the pro-inflammatory cascade via cytokine-JAK-STAT1/3 axis in liver.

Results

Hepatic NK Cells Are Activated in Mouse Models of NASH

We first examined hepatic NK cell function in experimental NASH. NASH was developed in methionine- and choline-deficient (MCD)-fed mice, with lipid accumulation and inflammation foci formation confirmed by H&E staining and Oil Red O staining (Figure 1A). Increased hepatic triglycerides (TG) contents and lipid peroxidation by thiobarbituric acid reactive substances (TBARs) assay and liver injury by elevated serum alanine aminotransferase (ALT) and aspartate aminotransferase (AST) levels were also observed (Table 1). The immune cell microenvironment in liver was analyzed by flow cytometry (Figure 1B). We found that the number of NK cells increased significantly (Table 2), along with increased infiltration of CD8⁺ T cell, monocytes derived macrophages (MoMF), and neutrophils in NASH liver of mice fed MCD compared with normal liver in mice fed control diet (Table 2). The NK cell surface markers including activating receptor NKG2D, degranulation marker CD107a, granzyme B, and cytokine interferon- γ (IFN- γ) were significantly increased, whereas inhibitory receptor NKG2A was decreased in NASH liver compared with the


normal control (Figure 1C), suggesting activated NK cell phenotype in NASH liver.

To verify the activated NK cell function in NASH, we established additional 2 experimental NASH in mice induced by choline-deficient high fat diet (CDHF) or STAM (Table 3). Consistent with MCD-induced NASH, NK cell number was increased significantly in CDHF and STAM-induced NASH (Table 4). Similarly, increased NK cell activating markers (NKG2D, CD107a, granzyme B, and IFN- γ) and decreased inhibitory marker NKG2A were observed in CDHF (Figure 1D) and STAM (Figure 1E) induced NASH. Aside from NK cells, expression of these function markers on NKT and T cells was also analyzed (Tables 5 and 6). Among these 3 models, no consistent activation of NKT and T cells was observed. Collectively, these results suggested that NK cells are activated in NASH liver, indicating the possible involvement of NK cells in NASH evolution.

NK Cell Deficiency Protects Mice From Experimental Steatohepatitis

To determine the functional significance of activated NK cells in NASH progression, NK cell deficient mice Nfil3^{-/-} and wild-type Nfil3^{+/+} littermates were fed with CDHF or normal chow for 18 weeks (Figure 2A). The absence of NK cells in Nfil3^{-/-} mice was verified by flow cytometry (Figure 2B). Compared with Nfil3^{+/+} littermates, Nfil3^{-/-} mice fed CDHF diet showed reduced lobular inflammation and less steatosis by H&E staining (Figure 2C). In line with the histology, decreased lipid accumulation in Nfil3^{-/-} mice was confirmed by reduced Oil Red O staining area (Figure 2C) and hepatic TG (Figure 2D). Moreover, reduction in hepatic TBARs, relative NADP⁺/nicotinamide adenine dinucleotide phosphate (NADPH) ratio (Figure 2D), and serum ALT and AST levels (Figure 2E) was demonstrated, inferring reduced hepatic lipid peroxidation and hepatocyte damage in Nfil3^{-/-} mice compared with Nfil3^{+/+} mice fed with CDHF diet. Nuclear factor kappa B (NF- κ B) activity was significantly decreased, which was evidenced by lower p-NF- κ B p65 protein level in Nfil3^{-/-} mice (Figure 2F). Immunofluorescence staining showed co-staining of DAPI and NF- κ B p65, indicating the nucleus

Abbreviations used in this paper: ALT, alanine aminotransferase; AST, aspartate aminotransferase; CDHF, choline-deficient high-fat diet; ELISA, enzyme-linked immunosorbent assay; FITC, fluorescein isothiocyanate; GM-CSF, granulocyte-macrophage colony-stimulating factor; HCC, hepatocellular carcinoma; IFN- γ , interferon gamma; Ig, immunoglobulin; IL12, interleukin 12; JAK-STAT, Janus kinase-signal transducer and activator of transcription; KEGG, Kyoto encyclopedia of genes and genomes; LPS, lipopolysaccharide; MCD, methionine- and choline-deficient; MFI, mean fluorescent intensity; MoMF, monocyte derived macrophage; NADPH, nicotinamide adenine dinucleotide phosphate; NAFLD, nonalcoholic fatty liver disease; NASH, nonalcoholic steatohepatitis; NF- κ B, nuclear factor kappa B; NK cell, natural killer cell; NKT cell, natural killer T cell; ROS, reactive oxygen species; TBARs, thiobarbituric acid reactive substances; TG, triglycerides.

 Most current article

© 2021 The Authors. Published by Elsevier Inc. on behalf of the AGA Institute. This is an open access article under the CC BY-NC-ND license (<http://creativecommons.org/licenses/by-nc-nd/4.0/>).

2352-345X

<https://doi.org/10.1016/j.jcmgh.2021.08.019>

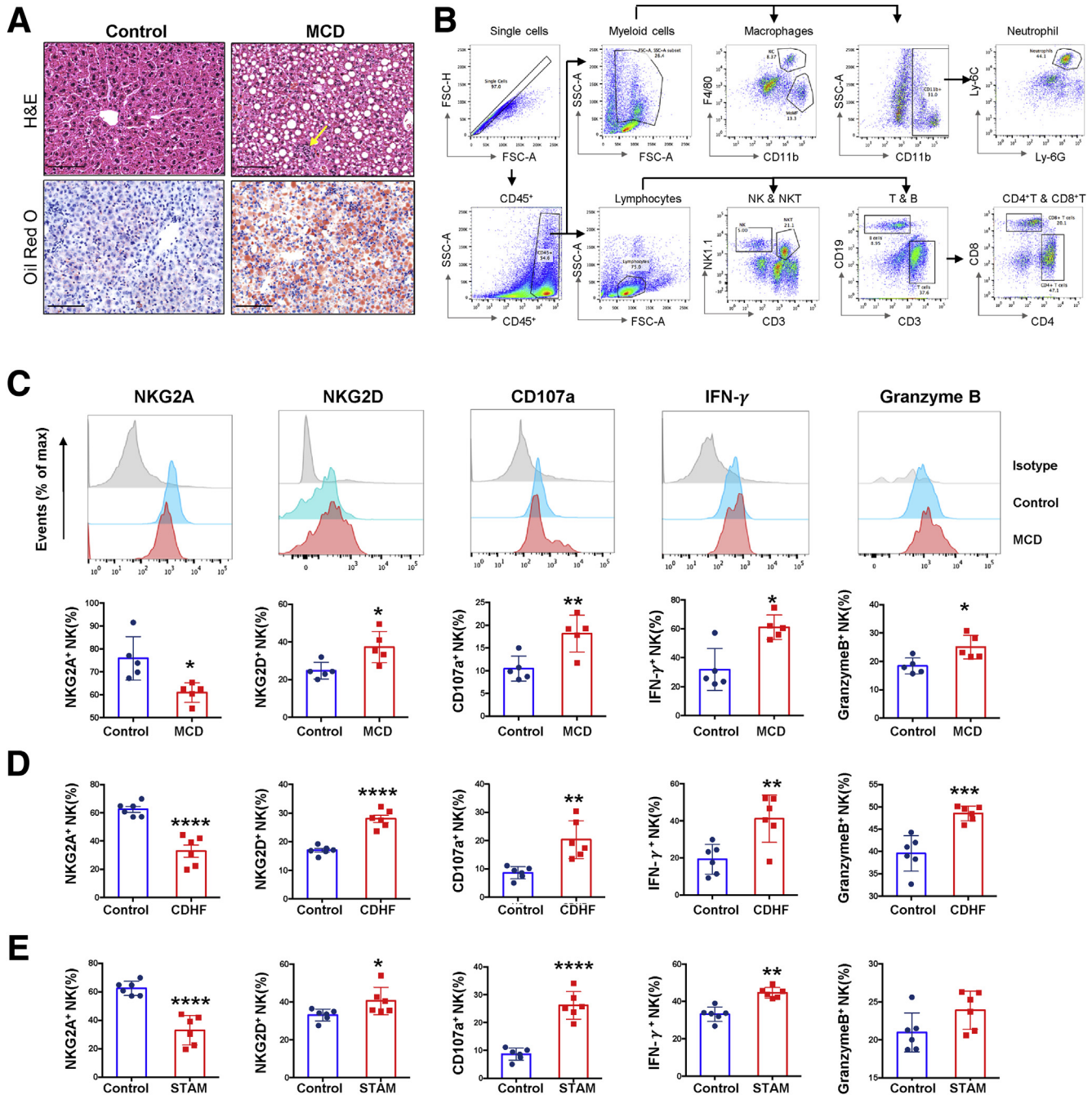


Figure 1. Hepatic NK cells are activated in mouse models of NASH. (A) Representative images of H&E staining and Oil Red O staining of mouse livers (arrows, inflammation cells). (B) Gating strategy for analysis of immune cell infiltration in liver by flow cytometry. (C) Representative histogram and expression levels of function molecular markers on liver NK cells in mice fed MCD or control diet (N = 5 per group). (D) Expression levels of function molecular markers on liver NK cells in mice fed CDHF or normal chow (N = 6 per group). (E) Expression levels of function molecular markers on liver NK cells in STAM model (N = 6 per group). Scale bars, 100 μ m. * P < .05, ** P < .01, *** P < .001, **** P < .0001.

translocation (Figure 2G). These findings were confirmed in MCD-induced NASH in *Nfil3*^{-/-} mice compared with *Nfil3*^{+/+} mice. *Nfil3*^{-/-} mice fed MCD showed improved liver histology with decreased necroinflammation score (Figure 3A), reduced hepatic TG, TBARS, relative NADP⁺/NADPH ratio (Figure 3B), as well as serum ALT and AST levels (Figure 3C). Moreover, decreased liver p-NF- κ B p65 protein

expression was identified in *Nfil3*^{-/-} mice (Figure 3D). Hepatic immune microenvironment was also analyzed in *Nfil3*^{-/-} mice. In both MCD- and CDHF-induced NASH, there were no significant differences in Kupffer cells, MoMFs, and neutrophils between *Nfil3*^{-/-} mice and wild-type mice (Table 7). These data suggested that phenotypes observed could be largely attributed by NK cell depletion.

Table 1. Histologic Information of MCD Induced Experimental NASH

	Control (N = 5)	MCD (N = 5)
Weight information		
Body weight (g)	28.77 ± 1.39	17.94 ± 0.71 ^d
Liver weight (g)	1.01 ± 0.06	0.63 ± 0.03 ^d
Liver to body weight ratio (%)	3.49 ± 0.15	3.51 ± 0.19
Histologic scores		
Steatosis	0.00 ± 0.00	2.15 ± 0.35 ^c
Necroinflammation	0.14 ± 0.10	2.15 ± 0.38 ^c
Biochemical analysis		
Hepatic TG (ng/mg tissue)	49.83 ± 6.76	93.62 ± 16.19 ^a
Hepatic TBARs (nmol/mg tissue)	1.11 ± 0.13	4.98 ± 0.33 ^d
Serum ALT (U/L)	74.2 ± 2.89	358.4 ± 29.79 ^d
Serum AST (U/L)	111.8 ± 17.77	301.4 ± 18.05 ^d

^aP < .05.^cP < .001.^dP < .0001 vs. control group.

Aside from immunity analysis, gut barrier, the dysfunction of which is regarded as one critical contributor to NASH pathogenesis, was also determined by serum lipopolysaccharide (LPS) analysis and fluorescence isothiocyanate (FITC)-dextran test (Table 8). In Nfil3^{+/+} mice, increased serum LPS and FITC-dextran concentration in MCD group suggested impaired gut barrier in NASH. For Nfil3^{-/-} mice, no obvious alternation in LPS and FITC-dextran level was observed in control diet group. In MCD feeding group, serum concentrations of LPS and FITC-dextran were both much lower compared with Nfil3^{+/+} mice, indicating alleviated gut barrier dysfunction in the absence of NK cells. This result is in accordance with alleviated NASH development, suggesting that liver NK cells mediated promoting effect play a dominant role. Taken together, these results suggested that NK cell deficiency protects mice against steatohepatitis development.

NK Cell Deficiency Suppresses Hepatic Pro-Inflammatory Cytokines and JAK/STAT Pathway in NASH

To understand the mechanism of ameliorated NASH progression in Nfil3^{-/-} mice, we compared the gene

expression profiles of liver tissues from Nfil3^{-/-} and Nfil3^{+/+} mice fed with MCD diet by RNA-sequencing analysis. As shown in Figure 4A, 108 genes were down-regulated and 62 genes were up-regulated in Nfil3^{-/-} mice compared with Nfil3^{+/+} mice. Majority of differentially expressed genes were cytokines. The down-regulated interleukin (IL) 1 β , IL6, IL12, IFN- γ , Ccl4, and Ccl5 in liver tissues of Nfil3^{-/-} mice were confirmed by real-time polymerase chain reaction (Figure 4B). Moreover, multiple pro-inflammatory cytokines and chemokines (IL12 [p40], CCL2, CCL3, CCL4, and CCL5) were significantly reduced in Nfil3^{-/-} mice compared with Nfil3^{+/+} mice by enzyme-linked immunosorbent assay (ELISA)-based cytokine profiling assay (Figure 4C). Using Kyoto encyclopedia of genes and genomes (KEGG) pathway enrichment analysis, multiple pro-inflammatory signaling pathways, including the Janus kinase-signal transducer and activator of transcription pathway (JAK-STAT), chemokine signaling and cytokine-cytokine receptor pathways, were blunted in Nfil3^{-/-} mice (Figure 4A). The reduced activity of JAK-STAT signaling was confirmed by decreased protein levels of p-STAT1 and p-STAT3 in Nfil3^{-/-} mice compared with Nfil3^{+/+} by Western blot (Figure 4D). These results collectively indicated that NK cell activation may contribute to the NASH progression via inducing hepatic pro-

Table 2. Hepatic Immune Microenvironment of MCD Induced NASH

Of CD45 ⁺ cells (%)	Control (N = 5)	MCD (N = 5)
NK cells	3.58 ± 0.59	6.28 ± 0.37 ^b
NKT cells	17.23 ± 1.16	9.97 ± 0.67 ^c
CD8 ⁺ T cells	15.34 ± 0.80	17.94 ± 1.32 ^a
Kupffer cells	6.93 ± 3.81	7.72 ± 0.82
MoMFs	4.40 ± 0.29	10.01 ± 1.18 ^b
Neutrophils	5.26 ± 0.83	11.18 ± 0.87 ^b

^aP < .05.^bP < .01.^cP < .001 vs. control group.

Table 3. Histologic Information of CDHF and STAM Induced NASH

NASH model	CDHF (N = 6 per group)		STAM (N = 6 per group)	
	Control	CDHF	Control	STAM
Weight information				
Body weight (g)	29.71 ± 1.52	46.42 ± 2.69 ^d	23.49 ± 0.33	19.79 ± 0.53 ^d
Liver weight (g)	1.62 ± 0.11	2.88 ± 0.63 ^d	1.04 ± 0.01	1.43 ± 0.06 ^d
L/B ratio (%)	5.44 ± 0.16	6.17 ± 1.15	4.54 ± 0.05	7.25 ± 0.35 ^d
Histologic scores				
Steatosis	0.00 ± 0.00	3.00 ± 0.00 ^d	0.00 ± 0.00	1.75 ± 0.19 ^d
Necroinflammation	0.14 ± 0.10	1.63 ± 0.49 ^d	0.14 ± 0.09	0.29 ± 0.08 ^a
Biochemical analysis				
Hepatic TG (ng/mg tissue)	49.83 ± 6.78	152.0 ± 7.66 ^d	24.03 ± 5.914	98.32 ± 11.44 ^c
Hepatic TBARs (nmol/mg tissue)	1.11 ± 0.13	6.54 ± 0.40 ^d	98.32 ± 11.44	4.17 ± 0.62 ^b
Serum ALT (U/L)	45.2 ± 3.29	136.4 ± 16.12 ^c	48.00 ± 3.882	93.83 ± 5.17 ^d
Serum AST (U/L)	70.46 ± 6.06	190.1 ± 30.44 ^a	55.83 ± 3.807	137.7 ± 7.89 ^d

L/B ratio, liver to body weight ratio.

^aP < .05.^bP < .01.^cP < .001.^dP < .0001 vs. control group.

inflammatory cytokines/chemokines and activating pro-inflammatory signaling pathways.

Activated NK Cells Isolated From Liver Secrete Pro-Inflammatory Cytokines

To confirm NK cell activation contributing to the NASH progression, we further evaluated the cytokines secreted from activated NK cells in NASH liver. We compared the cytokine and chemokine profiles of primary NK cells purified from NASH liver and normal liver by cytokine profiling assay (Figure 5A). NK cells isolated from NASH liver induced by MCD diet showed significantly elevated production of pro-inflammatory cytokines and chemokines, including IFN- γ , IL1 α , IL1 β , IL6, IL12 (p40), IL12 (p70), CCL2, CCL3, CCL4, CCL5, and granulocyte-macrophage colony-stimulating factor (GM-CSF) compared with NK cells isolated from normal liver of mice fed with MCD control diet (Figure 5B). To further validate the robust cytokine secretion potency, intracellular staining flow cytometry was conducted, and results showed that the mean fluorescence intensity (MFI) of these cytokines in NK cells from NASH liver (NASH-NK) is much higher than that from control group (CTL-NK)

(Figure 5C). In keeping with these results, the mRNA levels of specific cytokine and activating markers also increased in NASH-NK compared with CTL-NK (Figure 5D). These results were further confirmed in the second NASH model induced by CDHF diet. NK cells isolated from CDHF-induced NASH liver secreted significantly enhanced IFN- γ , IL1 α , IL1 β , IL12 (p40), GM-CSF, CCL3, CCL4, and CCL5, compared with NK cells isolated from normal liver of mice fed normal chow (Figure 5E). Taken together, these findings suggested that activated NK cells in NASH exhibit significantly stronger cytokine secretion potential, therefore contributing to the pathogenesis of NASH.

NK Cells From NASH Liver Induce Hepatocyte Damage Through Up-Regulation of JAK-STAT Signaling

To validate that NK cells promote NASH progression via cytokine secretion, we investigated the direct effect of NK cell-derived cytokines on hepatocytes *in vitro* (Figure 6A). Primary hepatocytes isolated from healthy liver were treated with the supernatant of NK cells purified from either mouse healthy liver (CTL-NK^{sup}) or NASH liver (NASH-

Table 4. Hepatic Immune Microenvironment of CDHF and STAM Induced NASH Model

Of CD45 ⁺ cells (%)	Control (N = 6)	CDHF (N = 6)	STAM (N = 6)
NK cells	9.53 ± 1.56	15.47 ± 2.15 ^a	7.69 ± 0.47
NKT cells	14.04 ± 1.56	12.59 ± 2.32	10.53 ± 0.98
CD8 ⁺ T cells	16.40 ± 0.96	32.64 ± 6.43 ^a	19.83 ± 2.20 ^a
Kupffer cells	7.04 ± 0.83	5.05 ± 0.73	5.33 ± 0.77
MoMFs	3.92 ± 0.54	5.90 ± 0.66 ^a	6.01 ± 0.36 ^a
Neutrophils	5.07 ± 0.83	6.58 ± 1.05 ^a	5.50 ± 1.03

^aP < .05 vs. control group.

Table 5. NKT Cell Function Analysis in Different Experimental NASH Models

MFI	MCD (N = 5 per group)		CDHF (N = 6 per group)		STAM (N = 6 per group)	
	Control	MCD	Control	CDHF	Control	STAM
NKG2A	2773.24 ± 440.65	1802.7 ± 572.51 ^a	941.57 ± 311.23	714.95 ± 233.50	1416.67 ± 125.14	1217.50 ± 48.19
NKG2D	813.00 ± 214.84	1266.00 ± 336.47 ^a	587.83 ± 31.28	520.67 ± 32.10 ^b	733.33 ± 25.45	781.00 ± 37.65
CD107a	815.78 ± 272.62	2628.28 ± 1668.47 ^a	260.00 ± 53.66	305.17 ± 45.18	616.67 ± 178.68	387.67 ± 45.73
IFN-γ	3869.80 ± 453.35	4174.40 ± 1281.03	923.83 ± 99.04	935.00 ± 104.69	2456.17 ± 77.00	2277.00 ± 69.80
Granzyme B	714.40 ± 30.86	803.20 ± 74.45 ^a	348.50 ± 55.12	348.50 ± 36.31	2144.00 ± 85.45	1882.33 ± 112.45

^aP < .05.^bP < .01 vs. control group.

NK^{sup}). Primary hepatocytes treated with NASH-NK^{sup} showed a significantly increased reactive oxygen species (ROS) level, NADP⁺/NADPH ratio, and apoptosis rate (Figure 6B) compared with primary hepatocytes treated with CTL-NK^{sup}, inferring that NASH-NK^{sup} could cause hepatocyte damage. To confirm these findings, the mouse immortalized hepatocyte cell line AML12 was treated with CTL-NK^{sup} or NASH-NK^{sup}. Consistently, NASH-NK^{sup} increased ROS level, NADP⁺/NADPH ratio, and apoptosis rate (Figure 6C) in AML12 hepatocytes. Moreover, the mRNA levels of critical pro-inflammatory cytokines and oxidative stress markers Il6, Cxcl-10, inos, and gp91^{phox} were significantly up-regulated in primary hepatocytes (Figure 6D) and in AML12 hepatocytes (Figure 6E) treated with NASH-NK^{sup}, suggesting that NASH-NK^{sup} induces hepatocyte inflammatory damage. In addition, NASH-NK^{sup} treatment induced protein expressions of p-NF-κB p65, p-STAT1 and p-STAT3 (Figure 6F). Collectively, these results suggested that activated NK cells could directly induce hepatocyte oxidative stress, inflammatory damage, and JAK-STAT and NF-κB activation through producing pro-inflammatory cytokines.

Antibody-Dependent NK Cell Depletion Ameliorates NASH Progression in Mice

Having confirmed the role of NK cell activation in promoting NASH development *in vivo* and *in vitro*, we assessed the potential of modulating NK cells in NASH treatment

using antibody-dependent NK cell depletion. The NK cell depletion antibody, anti-NK1.1 (PK136), was intraperitoneally injected every 3 days along with MCD diet feeding (Figure 7A). NK cell number decreased significantly in liver upon PK136 treatment (Figure 7B). As anticipated, PK136 ameliorated NASH progression by significantly decreased NASH score and lipid accumulation under Oil Red O staining (Figure 7C), along with decreased levels of hepatic TG, lipid peroxidation by TBARS, and NADP⁺/NADPH ratio (Figure 7D). Consistently, decreased serum ALT and AST levels were observed in PK136 treatment group (Figure 7E). Moreover, PK136 significantly reduced protein levels of p-STAT1, p-STAT3, and p-NF-κB p65 by Western blot (Figure 7F). Also, hepatic pro-inflammatory cytokines IL12 (p40), CCL2, CCL3, CCL4, and CCL5 exhibited significant down-regulation in PK136 group compared with immunoglobulin (Ig) G group (Figure 7G). Collectively, these results further confirmed the role of NK cells in NASH progression, and antibody PK136-dependent NK cell depletion can attenuate NASH development.

Discussion

Considering that NK cells make up the predominant lymphocyte population in liver^{14,15} and inflammation is one major pathophysiology of NASH,⁷ we studied the role of NK cells in NASH evolution. In MCD-induced NASH in mice, the pro-inflammatory immune microenvironment was evidenced by increased population of CD8⁺ T cells,

Table 6. T-Cell Function Analysis in Different Experimental NASH Models

MFI	MCD (N = 5 per group)		CDHF (N = 6 per group)		STAM (N = 6 per group)	
	Control	MCD	Control	CDHF	Control	STAM
NKG2A	369.20 ± 173.14	347.00 ± 70.03	785.33 ± 381.78	612.50 ± 61.58	1202.83 ± 120.14	1030.83 ± 146.19
NKG2D	380.60 ± 100.51	499.40 ± 111.70	518.50 ± 38.61	402.00 ± 18.93 ^d	337.33 ± 48.04	311.00 ± 30.11
CD107a	870.40 ± 35.60	997.80 ± 113.22 ^a	216.67 ± 46.26	187.33 ± 31.71	490.83 ± 107.02	460.50 ± 91.28
IFN-γ	379.40 ± 47.51	365.40 ± 43.95	827.67 ± 164.68	819.33 ± 198.68	2743.33 ± 238.46	2409.00 ± 628.60
Granzyme B	688.80 ± 83.95	770.60 ± 37.30	272.00 ± 65.61	268.67 ± 71.17	1946.83 ± 224.41	1704.50 ± 165.17

^aP < .05.^dP < .0001 vs. control group.

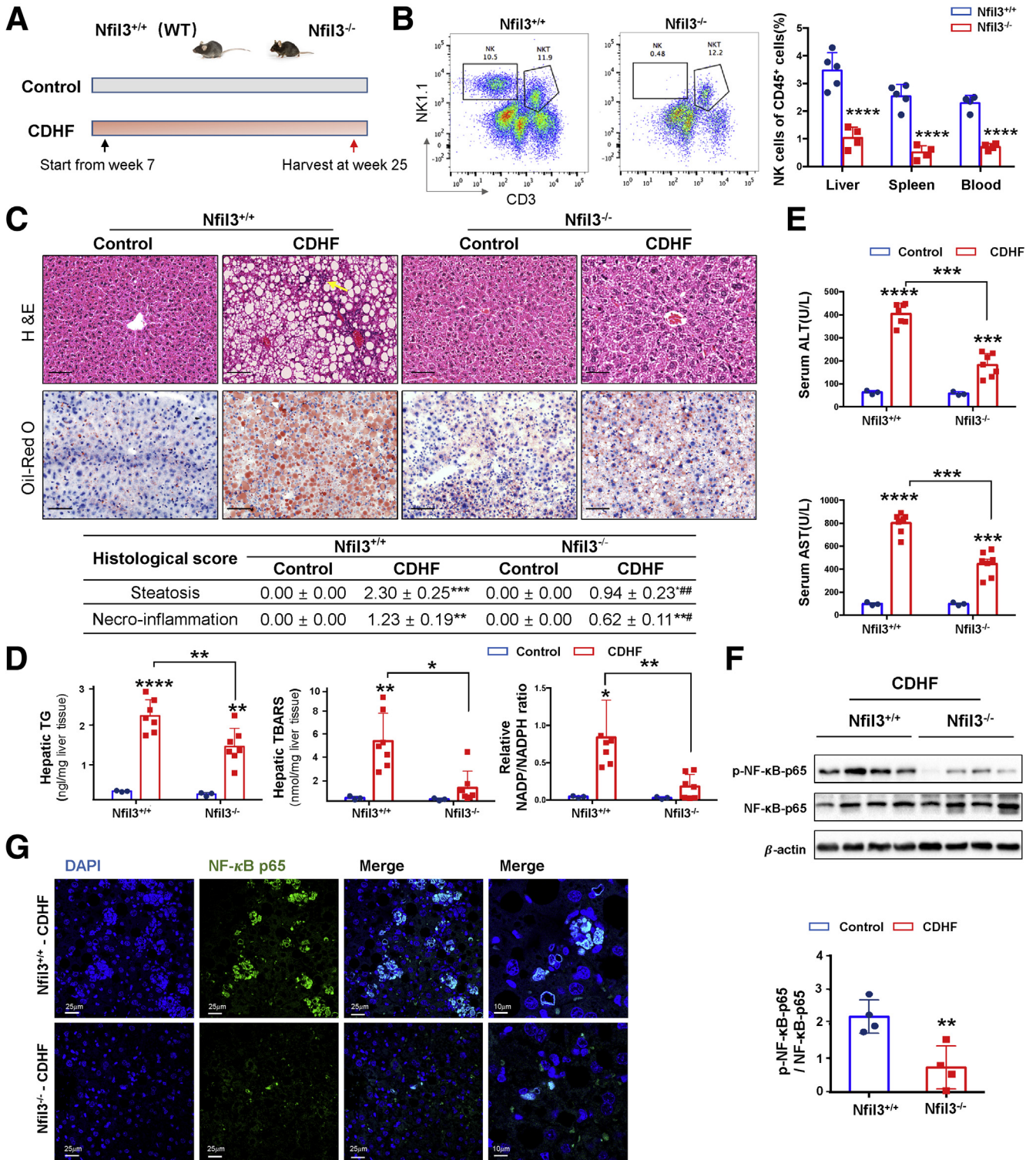


Figure 2. NK cell deficiency protects mice from CDHF induced experimental steatohepatitis. (A) Animal experiment design for Nfil3^{+/+} and Nfil3^{-/-} mice fed CDHF diet. (B) Representative FCM plots and NK cell population in Nfil3^{+/+} and Nfil3^{-/-} mice. (C) Representative images of H&E staining and Oil Red O staining of mouse liver (arrows, inflammation cells). Scale bars, 100 μ m. [#] $P < .05$, ^{##} $P < .01$ vs. Nfil3^{+/+} mice fed CDHF. (D) Hepatic TG, TBARS, and relative NADP⁺/NADPH ratio of Nfil3^{+/+} and Nfil3^{-/-} mice fed CDHF or control diet. (E) Serum ALT and AST levels in Nfil3^{+/+} and Nfil3^{-/-} mice fed CDHF or control diet. (F) Protein level of p-NF- κ B p65 in liver of Nfil3^{+/+} and Nfil3^{-/-} mice fed CDHF diet. (G) Representative images of immunofluorescence staining of NF- κ B p65. N = 3–7 per group. * $P < .05$, ** $P < .01$, *** $P < .001$, **** $P < .0001$. WT, wild-type.

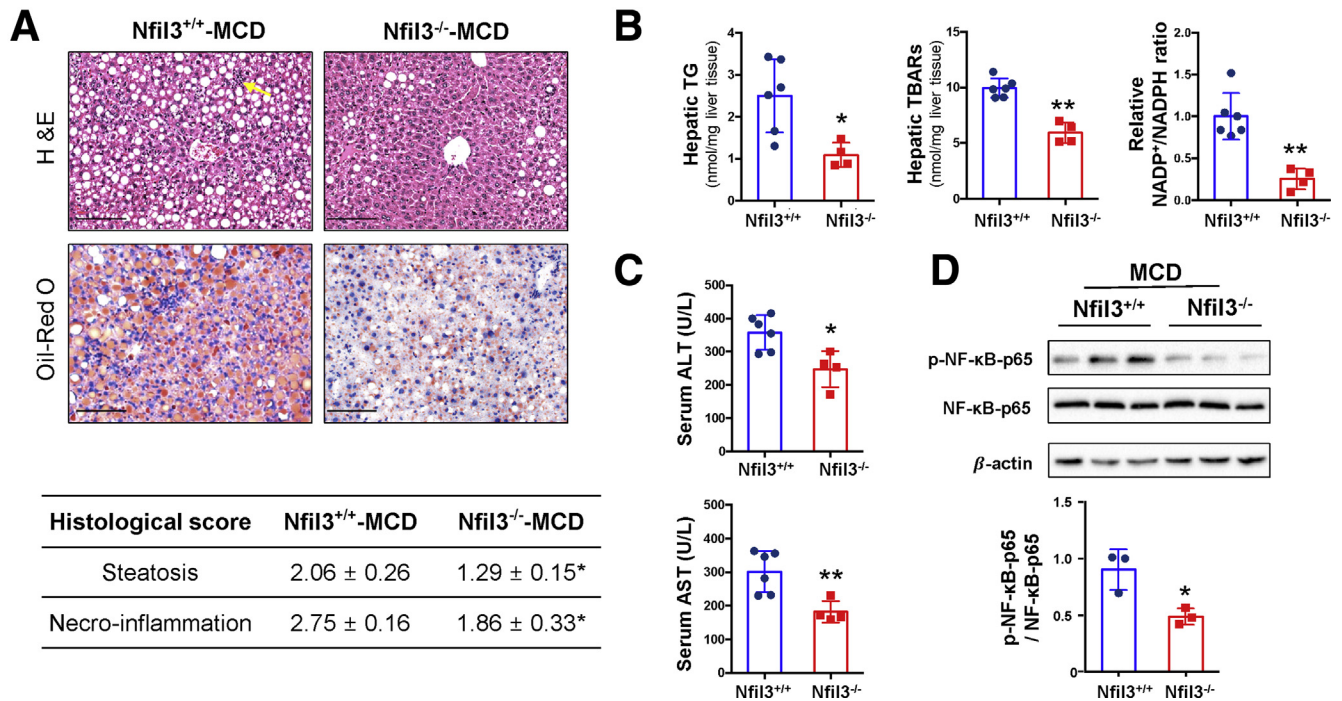


Figure 3. NK cell deficiency protects mice from MCD induced experimental steatohepatitis. (A) Representative images of H&E staining and Oil Red O staining of mouse liver (arrows, inflammation cells). (B) Hepatic TG, TBARS, and relative NADP⁺/NADPH ratio of Nfil3^{+/+} and Nfil3^{-/-} mice fed MCD diet. (C) Serum ALT and AST levels in Nfil3^{+/+} and Nfil3^{-/-} mice fed MCD diet. (D) Protein levels of p-NF-κB p65 in liver of Nfil3^{+/+} and Nfil3^{-/-} mice fed MCD diet. N = 4–6 per group. Scale bars, 100 μm. **P* < .05, ***P* < .01, ****P* < .001, *****P* < .0001.

macrophages, and neutrophils, which is consistent with previous reports.^{16,17} In particular, we identified the phenotypes of activated NK cells in NASH liver, which include significantly increased activating receptor NKG2D, effector maker CD107a, granzyme B, and cytokine IFN-γ, and decreased inhibitory marker NKG2A. This finding is consistent with previous study showing increased NKG2D⁺ NK cell population in the liver of NASH patients.¹⁸ We further established 2 additional experimental NASH induced by CDHF diet and STAM for validation, and consistent results among all 3 models thus confirmed the phenotypes of activated NK cells in mouse NASH liver. Taken together, NK cells were activated in experimental NASH liver, providing the initial evidence on the involvement of NK cell activation in the evolution of NASH.

To unveil the role of activated NK cells in the steatohepatitis progression, we established experimental NASH using NK cell deficiency mice Nfil3^{-/-} and wild-type Nfil3^{+/+} littermates. Attenuated liver steatohepatitis was observed in Nfil3^{-/-} mice with improved histology manifestation, decreased hepatic TG contents, lipid peroxides by TBARS and NADP⁺/NADPH ratio, and serum ALT and AST levels compared with Nfil3^{+/+} mice. Along with these findings, the key pro-inflammatory factor in NASH, NF-κB activation, was also suppressed as evidenced by decreased p-NF-κB p65 protein level in Nfil3^{-/-} mice compared with wild-type mice. In addition, nuclear translocation evidenced by the co-staining of DAPI and NF-κB p65 from immunofluorescence staining further validated the activation status of NF-κB p65

signaling. The NF-κB family of transcription factors can modulate multiple pro-inflammatory genes and is therefore regarded as the central player of immune response.¹⁹ Emerging evidence has verified the critical role of its activation in many inflammatory diseases including NAFLD.²⁰ Taken together, our findings inferred that liver NK cell activation exhibits pathogenic effect in the evolution of NASH.

The molecular mechanism behind NK cell activation-mediated NASH progression was investigated by RNA sequencing and cytokine profiling assay of the liver tissues from Nfil3^{-/-} and Nfil3^{+/+} mice. We found that multiple cytokines including IL12 (p40), CCL2, CCL3, CCL4, and CCL5 were significantly decreased in Nfil3^{-/-} mice compared with Nfil3^{+/+} mice. The differentially expressed genes were enriched in pro-inflammatory JAK-STAT, chemokine, cytokine, and T-cell receptor signaling pathways, which are inactivated in Nfil3^{-/-} mice. Inactivation of JAK-STAT signaling was confirmed by decreased protein expression of p-STAT1 and p-STAT3 in Nfil3^{-/-} mice compared with Nfil3^{+/+} mice. Considering the cytokine secretion function of NK cells and the critical role of cytokines in NASH development,²¹ alleviated steatohepatitis in Nfil3^{-/-} mice can be explained partly by decreasing cytokines that are due to the absence of NK cells and consequent inactivation of the pro-inflammatory JAK-STAT pathway.

To test the involvement of cytokines in NK cell-mediated NASH promoting effect, we characterized the cytokine profile of NK cells isolated from NASH liver. Compared with NK cells from normal liver, NK cells from NASH liver exhibited

Table 7. Analysis on Macrophages and Neutrophils in Livers of *Nfil3*^{-/-} Mice

Of CD45 ⁺ cell (%)	MoMF	Kupffer cell	Neutrophils
Control diet			
<i>Nfil3</i> ^{+/+} (N = 4)	3.97 ± 0.37	4.03 ± 0.97	1.52 ± 0.12
<i>Nfil3</i> ^{-/-} (N = 4)	5.71 ± 1.20	3.89 ± 0.88	3.82 ± 0.37 ^a
MCD diet			
<i>Nfil3</i> ^{+/+} (N = 7)	5.33 ± 0.92	5.08 ± 0.71	1.40 ± 0.21
<i>Nfil3</i> ^{-/-} (N = 4)	8.38 ± 1.60	4.55 ± 0.315	2.50 ± 0.70
CDHF diet			
<i>Nfil3</i> ^{+/+} (N = 7)	6.38 ± 0.86	15.29 ± 1.87	2.42 ± 0.33
<i>Nfil3</i> ^{-/-} (N = 7)	6.03 ± 1.14	11.45 ± 2.03	1.98 ± 0.29

^a*P* < .05 vs. *Nfil3*^{+/+} mice fed with same diet.

significantly higher cytokine secretion, including IFN- γ , IL1 β , IL6, IL12 (p40), IL12 (p70), CCL2, CCL3, CCL4, CCL5, and GM-CSF, which could contribute to the liver inflammatory immune microenvironment in NASH progression. Then intracellular staining flow cytometry was conducted to evaluate NK cell cytokine secretion potential *in vivo*. Consistent with ELISA-based cytokine profiling assay, higher MFI of identified cytokines in NASH-NK demonstrated enhanced cytokine secretion. Among these cytokines, IFN- γ , IL1 β , and IL6 are key pro-inflammatory cytokines in NASH.^{22–24} IL12 (p40) and IL12 (p70) are subunits of IL12, one kind of pro-inflammatory cytokine that belongs to the IL6 family.²⁵ IL12 is also one major stimulus of the JAK-STAT pathway, which was identified to be significantly suppressed in *Nfil3*^{-/-} mice fed with MCD or CDHF diet in this study. JAK-STAT is a popular transcription factor that receives extracellular stimulus and directly targets gene promoters in the nucleus, the well-accepted critical mediator in immune response.^{26,27} CCL2, CCL3, CCL4, and CCL5 are all CC chemokines that can recruit monocytes and other pro-inflammatory cells into the liver, driving immune response and fueling the pro-inflammatory microenvironment.^{28,29} Their increased expressions in NAFLD patients further validated their key contributions in the NAFLD pathogenesis.^{21,30} GM-CSF, previously defined as a critical growth factor for macrophage, now has been found to exert multiple functions in inflammation.³¹ It is another stimulus of JAK-STAT signaling and can recruit and promote maturation of dendritic cells, the well-acknowledged antigen presenting cells.³² In general, these cytokines and chemokines secreted by NK cells can fuel the pro-inflammatory microenvironment in liver. These findings thus confirmed the role of NK cell activation in promoting NASH progression through releasing a spectrum of key pro-inflammatory cytokines.

Having demonstrated that activated NK cells in NASH liver exhibit a strong cytokine secretion potential and played a promoting role in steatohepatitis, *in vitro* experiments were conducted to delineate the effect of cytokines released by activated NK cells from NASH liver on hepatocytes. Hepatocytes treated with supernatant derived from NK cells of NASH liver exhibited higher ROS production, NADP⁺/NADPH ratio, and early apoptosis rate, of which all these features are important triggers for NASH evolution.³³ Moreover, hepatocytes also showed enhanced protein expressions of p-STAT1, p-STAT3, and p-NF- κ B p65, indicating activation of JAK-STAT1/3 and NF- κ B p65 pro-inflammatory signaling and hepatocyte damage. JAK-STAT signaling plays a critical role in cellular homeostasis and immune response³⁴ and is involved in multiple liver diseases including virus hepatitis, NAFLD, and HCC.^{35–37} NF- κ B is activated in early stage of NASH and is an important pro-inflammatory mediator of NASH development.³⁸ Cooperation between STATs and NF- κ B or other transcription factors is believed to be present in driving gene expression and exerting biological function.³⁹ Collectively, these results further confirmed that NK cells are activated in experimental NASH and contribute to NASH development at least in part through inducing hepatocyte damage via cytokine-JAK-STAT1/3 axis and NF- κ B activation.

We finally conducted *in vivo* experiments designated to test the protective potential of NK cell neutralization against NASH. Substantial impaired steatohepatitis and suppressed serum levels of ALT and AST, hepatic oxidative stress, pro-inflammatory cytokines, JAK-STAT1/3 signaling, and NF- κ B activation were observed when treating MCD-fed mice with NK cell neutralization antibody PK136. These results further confirmed the critical role of NK cells in promoting NASH via cytokine-JAK-STAT1/3 axis. On the other hand, because

Table 8. Gut Barrier Function Analysis in MCD Fed *Nfil3*^{-/-} and Wild-type Mice

	Control			MCD		
	<i>Nfil3</i> ^{+/+} (N = 3)	<i>Nfil3</i> ^{-/-} (N = 3)	<i>P</i> value	<i>Nfil3</i> ^{+/+} (N = 3)	<i>Nfil3</i> ^{-/-} (N = 5)	<i>P</i> value
FITC dextran (mg/mL)	0.14 ± 0.05	0.12 ± 0.07	.8712	0.30 ± 0.07	0.09 ± 0.02	<.05
Serum LPS (ng/mL)	0.03 ± 0.02	0.04 ± 0.02	.9481	0.86 ± 0.07	0.33 ± 0.22	.0817

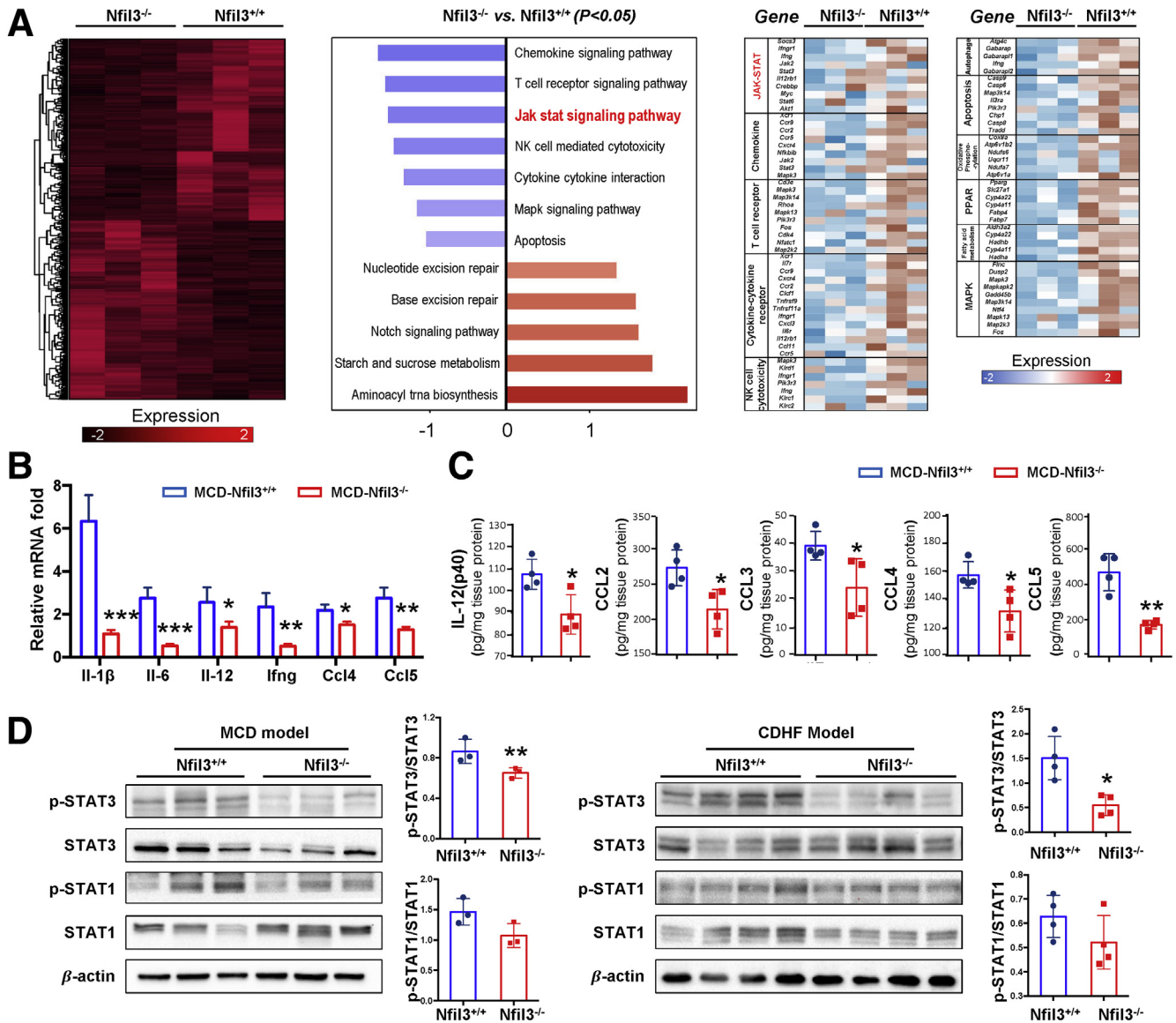


Figure 4. NK cell deficiency suppresses hepatic pro-inflammatory cytokines and JAK/STAT pathway in NASH. (A) Clusters of differentially expressed genes and KEGG pathway enrichment analysis in liver tissue of *Nfil3*^{+/+} and *Nfil3*^{-/-} mice fed MCD diet by RNA-sequencing data. (B) mRNA levels of *Il1β*, *Il6*, *Il12*, *Ifn-γ*, *Ccl4*, and *Ccl5* in liver tissue of *Nfil3*^{+/+} and *Nfil3*^{-/-} mice fed MCD diet. (C) Cytokine profiles of liver tissue from *Nfil3*^{+/+} and *Nfil3*^{-/-} mice fed MCD diet. (D) Protein levels of p-STAT1 and p-STAT3 in liver tissue of *Nfil3*^{+/+} and *Nfil3*^{-/-} mice fed MCD and CDHF diet. * $P < .05$, ** $P < .01$, *** $P < .001$, **** $P < .0001$.

of the blunted NASH evolution induced by PK136, it is rational to consider therapeutic translation of NK cell modulation in NASH. Further studies are needed to investigate NK cell modulation strategies for NASH prevention and therapy.

In conclusion, we identified the promoting effect of NK cell activation in the evolution of NASH. Activated NK cells in the NASH liver exhibited robust cytokine secretion potential and induced hepatocyte damage via cytokine-JAK-STAT1/3 axis, thereby contributing to steatohepatitis progression. Moreover, antibody-dependent NK cell neutralization significantly alleviated steatohepatitis in mice, providing a potential strategy for NK cell manipulation in NASH prevention.

Materials and Methods

Animals and Treatments

Male C57BL/6 mice (6–8 weeks) were fed with either MCD diet (MP Biomedicals, Irvine, CA) for 4 weeks or CDHF diet (Research Diet, New Brunswick, NJ) for 18 weeks. For the STAM model, male C57BL/6 mice were injected with 200 μg streptozotocin 2 days after birth and were fed with high-fat diet (Research Diet) starting from week 4. NASH became obvious at week 8. In the meantime, age-matched male mice fed with MCD control diet or normal chow were set as control groups.

NK cells knockout mice *Nfil3*^{-/-} (provided by Prof. Tak Wah Mak, Toronto University and Prof Dong Zhongjun,

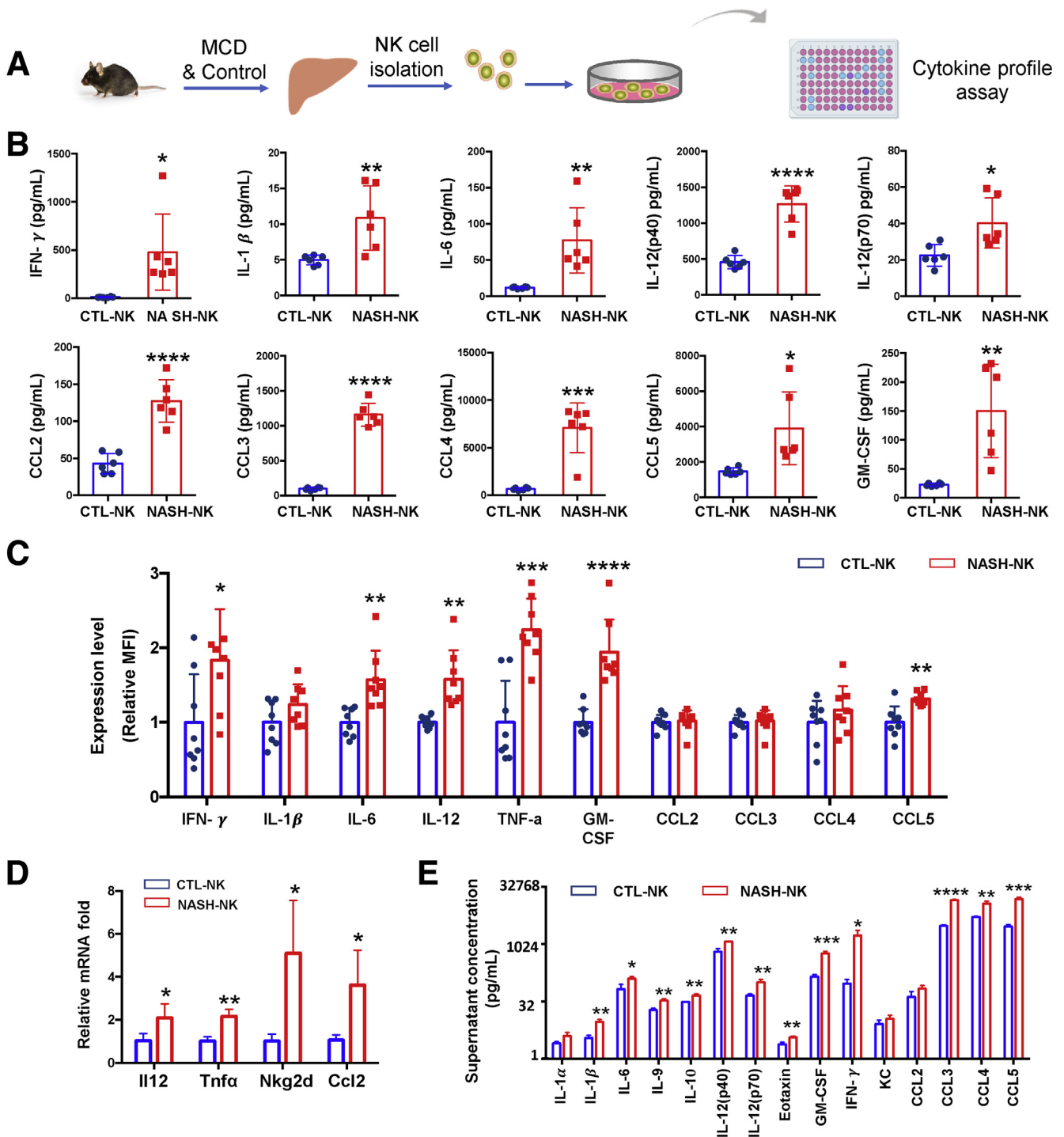


Figure 5. Activated NK cells isolated from NASH liver secrete pro-inflammatory cytokines. (A) Schematic diagram for analysis of primary NK cells derived cytokine. (B) Cytokine milieu of liver NK cells from control (CTL-NK) and MCD groups (NASH-NK). (C) Relative MFI of identified cytokines in NK cells from control (CTL-NK) and MCD groups (NASH-NK), $N = 8$ per group. (D) mRNA levels of *Il12*, *Tnfa*, *Ccl2*, and *Nkg2d* in NK cells isolated from the control liver and NASH liver. (E) Cytokine milieu of liver NK cells from control group and CDHF group. * $P < .05$, ** $P < .01$, *** $P < .001$, **** $P < .0001$.

Tsinghua University) and age-matched C57BL/6 wild-type littermates (*Nfil3*^{+/+}) were fed with either MCD or its corresponding control diet for 4 weeks or CDHF diet/normal chow for 18 weeks to establish steatohepatitis.

For NK cell depletion *in vivo*, male C57BL/6 mice were given NK cell neutralization antibody (anti-NK1.1, PK136)

or isotype-matched rat IgG2 α monoclonal antibody control (BioLegend, San Diego, CA) by intraperitoneal injection (150 μ g in 200 μ L phosphate-buffered saline per mouse) every 3 days along with MCD diet feeding.

All mice were fasted before harvest. Weights of liver were recorded. Serum and liver tissues were collected for

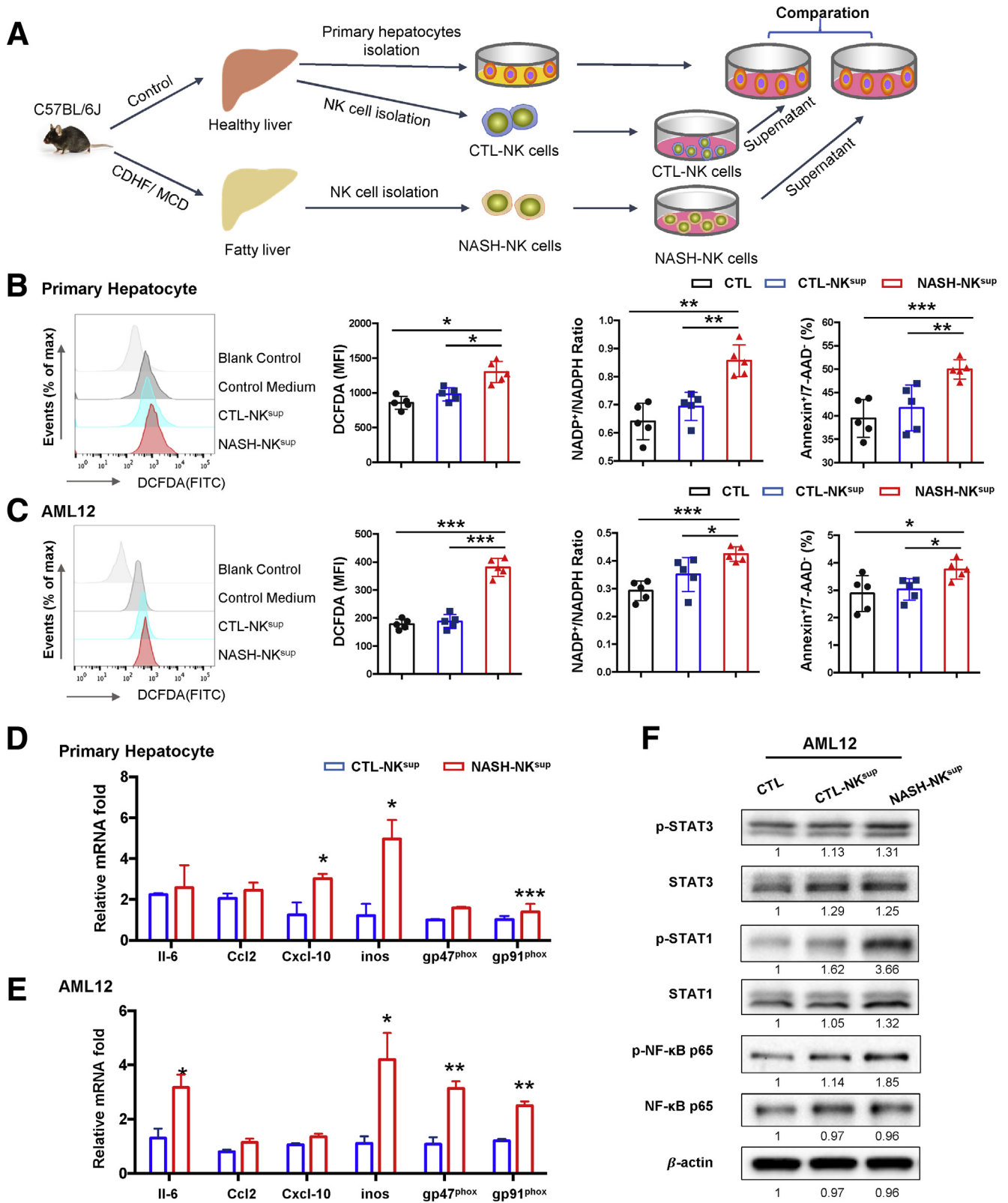


Figure 6. NK cells from NASH liver induce hepatocyte damage through up-regulation of JAK-STAT signaling. (A) Schematic diagram of NK cells derived supernatant treatment on hepatocytes. (B) Representative histogram and quantification of ROS level, NADP⁺/NADPH ratio, and Annexin V⁺7-AAD⁻ hepatocytes proportion after NK cells derived supernatant treatment. (C) Representative histogram and quantification of ROS level, NADP⁺/NADPH ratio, and Annexin V⁺7-AAD⁻ AML12 proportion after NK cells derived supernatant treatment. (D) mRNA levels of pro-inflammatory cytokines (Il6, Ccl2, Cxcl-10) and stress associated markers (inos, gp47^{phox}, gp91^{phox}) in primary hepatocytes after NK cells derived supernatant treatment. (E) mRNA levels of pro-inflammatory cytokines (Il6, Ccl2, Cxcl-10) and stress associated markers (inos, gp47^{phox}, gp91^{phox}) in AML12 after NK cells derived supernatant treatment. (F) Protein levels of p-STAT1, p-STAT3, and p-NF-κB p65 in AML12 treated with NK cells derived supernatant. Individual experiments were repeated 3 times; results represent data from representative experiment. *P < .05, **P < .01, ***P < .001.

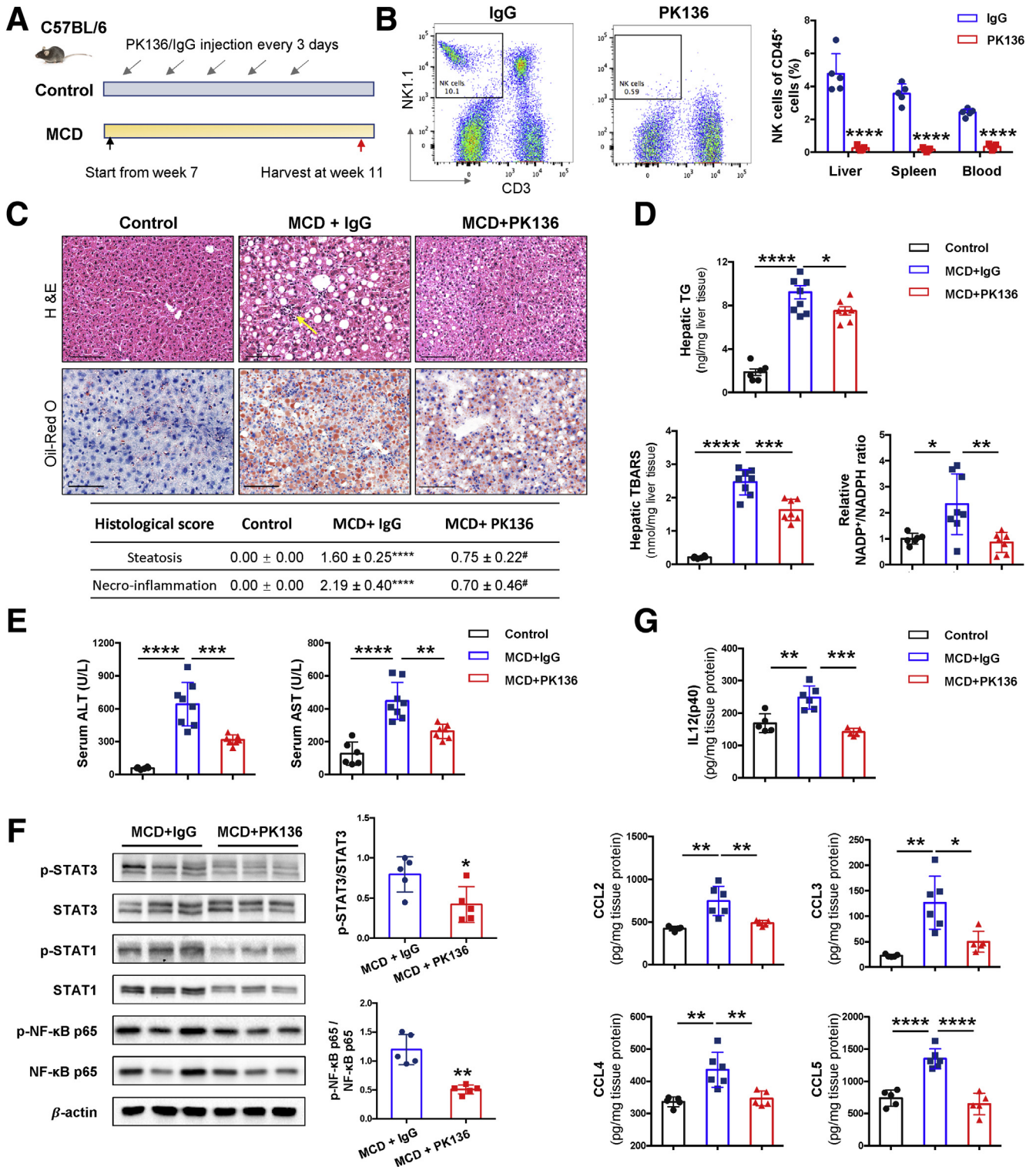


Figure 7. Antibody-dependent NK cell depletion ameliorates NASH progression in mice. (A) Schematic diagram of PK136 and IgG control treatment for MCD-induced mouse NASH. (B) Representative FCM plots and NK cell population of mice treated with PK136 and IgG control. (C) Representative images of H&E staining and Oil Red O staining of mouse liver (arrows, inflammation cells). #*P* < .05 vs. MCD fed mice treated with IgG. (D) Hepatic TG, TBARS, and relative NADP⁺/NADPH ratio of mice fed MCD diet with IgG or PK136 treatment. (E) Serum ALT and AST levels of mice fed MCD diet with IgG or PK136 injection. (F) Protein levels of p-STAT1, p-STAT3, and p-NF-κB p65 in liver of MCD fed mice treated with IgG control or PK136. (G) Cytokine profiles of liver tissue of MCD fed mice treated with IgG control or PK136. N = 5–7 per group. Scale bars, 100 μm. **P* < .05, ***P* < .01, ****P* < .001, *****P* < .0001.

further analysis. All animals received humane care, and all animal studies were performed in accordance with guidelines approved by the Animal Experimentation Ethics Committee of the Chinese University of Hong Kong.

Isolation of Leukocytes, NK Cells, and Hepatocytes

For isolation of liver leukocytes, fresh liver tissue was gently ground on a 70 μ m cell strainer (BD Biosciences, San Jose, CA) in phosphate-buffered saline with 1% bovine serum albumin until uniform cell suspensions were obtained. Then cell pellets were resuspended in 40% Percoll (GE Healthcare, Chicago, IL) and gently layered over 70% Percoll gradient with centrifugation for 30 minutes at 1260g. Leukocytes were obtained from the interface layer. To isolate leukocytes from

spleen, spleens were ground and filtered through 70 μ m cell strainer. Leukocytes were obtained after lysis of red blood cells using RBC lysis buffer (BioLegend).

Purified NK cells were isolated from the liver leukocytes by mouse NK cell isolation kit (Miltenyi Biotec, Bergisch Gladbach, Germany). By negative selection, leukocytes were stained with a cocktail of biotin-conjugated antibodies and anti-biotin microbeads, and unlabeled NK cells could be purified via depleting non-target cells.

Primary hepatocytes were isolated from male C57BL/6 mice as previously described.⁴⁰ Briefly, *in situ* liver perfusion was performed with ethylene glycol tetraacetic acid (EGTA) buffer, followed by collagenase (Sigma-Aldrich, St Louis, MO). The primary hepatocytes were obtained after mechanical and density-based separation. Finally, hepatocytes were counted

Table 9. Antibodies Used in This Study

Antibody	Cat. no.	Company
Phospho-Stat1 (Tyr701) (58D6)	#9167	Cell Signaling
STAT1	#9172P	Cell Signaling
Phospho-Stat3(Tyr705) (M9C6)	#4113	Cell Signaling
Phospho NF- κ B p65	#3031	Cell Signaling
NF- κ B p65	#8242	Cell Signaling
β -actin	#4970	Cell Signaling
STAT3	SC-482	Santa Cruz
Anti-mouse CD107a (LAMP1) FITC	121606	BioLegend
Anti-mouse CD11b (M1/70) PE- Cy5	101210	BioLegend
Anti-mouse CD19 (6D5) PE- Cy5	115508	BioLegend
Anti-mouse CD3 (17A2) PE	100206	BioLegend
Anti-mouse CD3 (17A2) PE-Cy7	100220	BioLegend
Anti-mouse CD4 (GK1.5) PE-Cy7	100422	BioLegend
Anti-mouse CD45(30-F11) BV605	103155	BioLegend
Anti-mouse CD8(53-6.7) FITC	100706	BioLegend
Anti-mouse F4/80 (BM8) FITC	123108	BioLegend
Anti-mouse IFN-g (XMG1.2) PerCP-CY5.5	505822	BioLegend
Anti-mouse IL-12/IL-23 p40 (C15.6) PerCP/Cyanine5.5	505211	BioLegend
Anti-mouse IL-6 (MP5-20F3) PE	504503	BioLegend
Anti-mouse GM-CSF (MP1-22E9) FITC	505403	BioLegend
Anti-mouse Ly-6G (1A8) PE	127612	BioLegend
Anti-mouse Ly-6C (HK1.4) PE-Cy7	128018	BioLegend
Anti-mouse/rat/human MCP-1 PE	505903	BioLegend
Anti-mouse MHCII BV421	107632	BioLegend
Anti-mouse NK1.1(PK136) BV421	108732	BioLegend
Anti-mouse RANTES (CCL5) PerCP/Cyanine5.5	515507	BioLegend
Anti-mouse CD27 (LG.3A10) BV605	563365	BD
Anti-mouse NKG2D (CX5) BV711	563694	BD
Anti-mouse CCL3 (MIP-1 alpha) (DNT3CC), PE	12-7532-80	eBioscience
Anti-mouse Granzyme B (16G6) PE	12-8822	eBioscience
Anti-mouse IL-1 beta (NJTEN3) FITC	11-7114-80	eBioscience
Anti-mouse Ly-6G/Ly-6C (Gr-1) PE-Cy5	12-8898-82	eBioscience
Anti-mouse NKG2A (16A11) PE	12-5897	eBioscience
Anti-mouse perforin (eBioOMAK-D) FITC	11-9392-82	eBioscience
Purified anti-mouse NK-1.1 antibody (PK136)	108758	BioLegend
Purified mouse IgG2a, κ isotype Ctrl antibody	400281	BioLegend

Table 10. Primers Used in This Study

Gene	Primer	Sequence
For quantitative polymerase chain reaction		
<i>Ccl2</i>	Forward	TTAAAAACCTGGATCGGAACCAA
	Reverse	GCATTAGCTTCAGATTACGGGT
<i>Ccl3</i>	Forward	ACTGCCTGCTGCTTCTCCTACA
	Reverse	ATGACACCTGGCTGGGAGCAAA
<i>Ccl4</i>	Forward	ACCCTCCCCTTCTGCTGTTT
	Reverse	CTGTCTGCCTCTTTTGGTCAGG
<i>Ccl5</i>	Forward	CCC CCG CAC CTG CCT CAC CAT A
	Reverse	AGG CAG CGC GAG GGA GAG GTA
<i>Il1b</i>	Forward	CCGGAGACCCTTAGATCGA
	Reverse	TAGCCTGTAAAAGATTTCTGCAAACC
<i>Il6</i>	Forward	CCAGAGATACAAAGAAATGATGG
	Reverse	ACTCCAGAAGACCAGAGGAAAT
<i>Il10</i>	Forward	GGTGAGAAGCTGAAGACCCT
	Reverse	TGTCTAGGTCTGGAGTCCA
<i>Il12</i>	Forward	CCAGAGACATGGAGTCATAG
	Reverse	AGATGTGAGTGGCTCAGAGT
<i>Il12 (p40)</i>	Forward	CAGAAGCTAACCATCTCCTGGTTTG
	Reverse	TCCGGAGTAATTTGGTGCCTCACAC
<i>Tnfa</i>	Forward	CCAGACCCTCACACTCAGATC
	Reverse	CACTTGGTGGTTTGCTACGAC
<i>Ifng</i>	Forward	CTCTTCTCATGGCTGTTTC
	Reverse	CACCATCCTTTTGCCAGT
<i>Nkg2d</i>	Forward	AGTTGAGTTGAAGGCTTTGACTC
	Reverse	ACTTTGCTGGCTTGAGGTC
<i>Cxcl-10</i>	Forward	TCATCCCTGCGAGCCTATCC
	Reverse	TGCGTGGCTTCACTCCAGTT
<i>actin</i>	Forward	CCACTGTCGAGTCGCGTCC
	Reverse	ATCCCACCATCACACCCTGG
<i>gp47^{phox}</i>	Forward	TTCCATCCCCAAATGCAAAG
	Reverse	TCAGATGCCCTAAAACCGGAG
<i>gp91^{phox}</i>	Forward	GACCATTGCAAGTGAACACCC
	Reverse	AAATGAAGTGGACTCCACGCG
<i>inos</i>	Forward	ATTCACAGCTCATCCGGTACG
	Reverse	GGATCTTGACCATCAGCTTGC
For genotyping		
<i>Nfil3^{-/-} transgenic mice</i>	Neo 469 Ex2, 1659L Seg05	TAG CCG GAT CAA GCG TAT GC ACA CCC AGA CAG ACG CCG TT GCC TTA CCG CAC AAG CTT CG

and plated on collagen-coated plates for 3 hours and then changed with Williams E medium supplemented with 10% fetal bovine serum (ATCC, Manassas, VA) and penicillin-streptomycin solution for further experiment.

Multi-Color Flow Cytometry Analysis

The isolated leukocytes were incubated with rat immunoglobulin for 30 minutes for Fc receptors blockade. Then the cells were stained with fluorescence antibodies for 30 minutes at 4 °C. For CD107a and intracellular staining, leukocytes were incubated with RPMI-1640 medium supplemented with phorbol 12-myristate 13-acetate (PMA) (50 ng/mL; Sigma-Aldrich), ionomycin (1 mg/mL; Sigma-Aldrich), monensin (10 ng/mL; Sigma-Aldrich), and FITC-

CD107a for 4 hours at 37°C in a 5% CO₂ incubator, followed by surface marker staining. After fixation and permeabilization via the Intracellular Fixation & Permeabilization Buffer Set (Thermo Fisher Scientific, Waltham, MA), cells were stained for intracellular molecules. The fluorescent antibodies and primers used in this study are shown in Tables 9 and 10, respectively. Data were acquired on BD FACSCelesta flow cytometer (BD Biosciences, San Jose, CA) and analyzed with FlowJo software (Treestar Inc, San Carlos, CA).

NK Cell Derived Supernatant Treatment

After isolation and cell counting, same amount of NK cells isolated from healthy and NASH livers were seeded on

the 48-well plate and cultured for 24 hours. The supernatants were then collected for *in vitro* experiment. Primary hepatocytes and hepatocyte cell line AML12 were seeded on 12-well plates and treated with control medium supplemented with supernatants of NK cells isolated from healthy or NASH livers. After treatment for 24 hours, cell pellets were collected for further analysis. Individual experiments were repeated at least 3 times, and results present data from representative experiment.

ROS Analysis

Cellular ROS level was analyzed by using DCFDA/H2DCFDA-Cellular ROS Assay Kit (Abcam, Cambridge, MA) according to manufacturer's instructions. Briefly, after treatment, cells were harvested and stained with 20 $\mu\text{mol/L}$ DCFDA in culture medium at 37°C. After 30 minutes of incubation, ROS level was measured by flow cytometer immediately. The experiments were performed 3 times. Results were shown as means \pm standard deviation.

NADP⁺/NADPH Ratio

NADP⁺/NADPH ratios in cells and tissues were quantified by the NADP⁺/NADPH Assay Kit (Abcam) according to the manufacturer's instructions. Total NADPH was extracted from cell pellets (2×10^6) or tissues (30 mg) using the NADP⁺/NADPH extraction buffer. For NADPH, an additional decomposition step is performed as 200 μL extracted samples were heated at 60°C for 30 minutes. After incubation with the provided reaction mix, multiple readings were taken by colorimetric microplate reader. All individual experiments were conducted 3 times. Results are shown as means \pm standard deviation.

Cytokine Profile Assay

To analyze cytokine secretion of primary NK cells, same amounts of NK cells (2×10^5 per well) were seeded on 96-well plate with RPMI-1640 supplied with 10% fetal bovine serum, penicillin-streptomycin solution, and IL2 (200 UI/mL) (PeproTech, Cranbury, NJ). After 24-hour culture, supernatants were collected for cytokine profile analysis using Bio-Plex Pro Mouse Cytokine 23-plex Assay (Bio-Rad, Hercules, CA) according to the manufacturer's instructions.

For liver tissue cytokine analysis, tissue proteins were extracted using the CytoBuster Protein Extraction Kit (Novagen, Austin, TX) containing protease inhibitors (Roche, Basel, Switzerland) and phosphatase inhibitors (Roche). The protein concentration was determined by BCA protein assay (Thermo Fisher) and adjusted to 500 $\mu\text{g/mL}$ before analysis with the sample diluent supplied in the Bio-Plex Pro Mouse Cytokine 23-plex Assay kit.

LPS Analysis

Serum LPS level was determined by Mouse LPS ELISA Kit (Cusabio, Houston, TX; CSB-E13066m) according to the manufacturer's instructions. Briefly, serum was diluted to suitable folds and added to the wells with standards provided by the kit; LPS in samples are bound by immobilized

antibody. After removing the unbound substances, biotin-conjugated antibodies specific to LPS are added. After wash and avidin conjugated horseradish peroxidase incubation step, a substrate solution is added, and color develops in proportion to amount of LPS.

FITC-Dextran Based Intestinal Permeability Detection

FITC-dextran based gut permeability test was performed before mouse harvest. Briefly, after 3 hours fasting, mice were administrated 80 mg/mL 4 kDa FITC-dextran at a volume of 150 μL by oral gavage; tail vein blood was collected 4 hours after the gavage. Standards (range, 0.08–267 $\mu\text{g/mL}$) were obtained by diluting the FITC-dextran gavage solution in phosphate-buffered saline. One hundred μL of diluted serum samples, standards, as well as blanks (phosphate-buffered saline and diluted serum from untreated animals) were added to black 96-well microplates. FITC-dextran concentration was determined from the readings taken by fluorescence spectrophotometer at an excitation wavelength of 485 nm and an emission wavelength of 528 nm.

Statistical Analysis

Data were expressed as mean \pm standard deviation. Mann-Whitney *U* test or Student *t* test was used to compare the differences between 2 groups. All statistical analyses were performed using GraphPad Prism 7.0 Software (GraphPad, La Jolla, CA). A difference at $P < .05$ was considered as statistically significant.

All authors had access to the study data and had reviewed and approved the final manuscript.

References

1. Younossi Z, Anstee QM, Marietti M, Hardy T, Henry L, Eslam M, George J, Bugianesi E. Global burden of NAFLD and NASH: trends, predictions, risk factors and prevention. *Nat Rev Gastroenterol Hepatol* 2018; 15:11–20.
2. Anstee QM, Reeves HL, Kotsiliti E, Govaere O, Heikenwalder M. From NASH to HCC: current concepts and future challenges. *Nat Rev Gastroenterol Hepatol* 2019;16:411–428.
3. Eslam M, Newsome PN, Sarin SK, Anstee QM, Targher G, Romero-Gomez M, Zelber-Sagi S, Wai-Sun Wong V, Dufour JF, Schattenberg JM, Kawaguchi T, Arrese M, Valenti L, Shiha G, Tiribelli C, Yki-Jarvinen H, Fan JG, Gronbaek H, Yilmaz Y, Cortez-Pinto H, Oliveira CP, Bedossa P, Adams LA, Zheng MH, Fouad Y, Chan WK, Mendez-Sanchez N, Ahn SH, Castera L, Bugianesi E, Ratziu V, George J. A new definition for metabolic dysfunction-associated fatty liver disease: an international expert consensus statement. *J Hepatol* 2020;73:202–209.
4. Dhanasekaran R, Felsher DW. A tale of two complications of obesity: NASH and hepatocellular carcinoma. *Hepatology* 2019;70:1056–1058.

5. Brunt EM, Wong VW, Nobili V, Day CP, Sookoian S, Maher JJ, Bugianesi E, Sirlin CB, Neuschwander-Tetri BA, Rinella ME. Nonalcoholic fatty liver disease. *Nat Rev Dis Primers* 2015;1:15080.
6. Ioannou GN. The role of cholesterol in the pathogenesis of NASH. *Trends Endocrinol Metab* 2016;27:84–95.
7. Schuster S, Cabrera D, Arrese M, Feldstein AE. Triggering and resolution of inflammation in NASH. *Nat Rev Gastroenterol Hepatol* 2018;15:349–364.
8. Machado MV, Diehl AM. Pathogenesis of nonalcoholic steatohepatitis. *Gastroenterology* 2016;150:1769–1777.
9. Younossi ZM. Non-alcoholic fatty liver disease: a global public health perspective. *J Hepatol* 2019;70:531–544.
10. Wolf MJ, Adili A, Piotrowitz K, Abdullah Z, Boege Y, Stemmer K, Ringelhan M, Simonavicius N, Egger M, Wohlleber D, Lorentzen A, Einer C, Schulz S, Clavel T, Protzer U, Thiele C, Zischka H, Moch H, Tschop M, Tumanov AV, Haller D, Unger K, Karin M, Kopf M, Knolle P, Weber A, Heikenwalder M. Metabolic activation of intrahepatic CD8⁺ T cells and NKT cells causes nonalcoholic steatohepatitis and liver cancer via cross-talk with hepatocytes. *Cancer Cell* 2014;26:549–564.
11. Kazankov K, Jorgensen SMD, Thomsen KL, Moller HJ, Vilstrup H, George J, Schuppan D, Gronbaek H. The role of macrophages in nonalcoholic fatty liver disease and nonalcoholic steatohepatitis. *Nat Rev Gastroenterol Hepatol* 2019;16:145–159.
12. Mikulak J, Bruni E, Oriolo F, Di Vito C, Mavilio D. Hepatic natural killer cells: organ-specific sentinels of liver immune homeostasis and physiopathology. *Front Immunol* 2019;10:946.
13. Shi FD, Ljunggren HG, La Cava A, Van Kaer L. Organ-specific features of natural killer cells. *Nat Rev Immunol* 2011;11:658–671.
14. Gao B, Jeong WI, Tian Z. Liver: an organ with predominant innate immunity. *Hepatology* 2008;47:729–736.
15. Rehermann B. Pathogenesis of chronic viral hepatitis: differential roles of T cells and NK cells. *Nat Med* 2013;19:859–868.
16. Gadd VL, Skoien R, Powell EE, Fagan KJ, Winterford C, Horsfall L, Irvine K, Clouston AD. The portal inflammatory infiltrate and ductular reaction in human nonalcoholic fatty liver disease. *Hepatology* 2014;59:1393–1405.
17. Miura K, Yang L, van Rooijen N, Ohnishi H, Seki E. Hepatic recruitment of macrophages promotes nonalcoholic steatohepatitis through CCR2. *Am J Physiol Gastrointest Liver Physiol* 2012;302:G1310–G1321.
18. Stiglund N, Strand K, Cornillet M, Stal P, Thorell A, Zimmer CL, Naslund E, Karlgren S, Nilsson H, Mellgren G, Ferno J, Hagstrom H, Bjorkstrom NK. Retained NK cell phenotype and functionality in non-alcoholic fatty liver disease. *Front Immunol* 2019;10:1255.
19. Liu T, Zhang L, Joo D, Sun SC. NF-kappaB signaling in inflammation. *Signal Transduct Target Ther* 2017;2.
20. Zhang T, Hu J, Wang X, Zhao X, Li Z, Niu J, Steer CJ, Zheng G, Song G. MicroRNA-378 promotes hepatic inflammation and fibrosis via modulation of the NF-kappa B-TNF alpha pathway. *J Hepatol* 2019;70:87–96.
21. Pan X, Chiwanda Kaminga A, Liu A, Wen SW, Chen J, Luo J. Chemokines in non-alcoholic fatty liver disease: a systematic review and network meta-analysis. *Front Immunol* 2020;11:1802.
22. Park EJ, Lee JH, Yu GY, He G, Ali SR, Holzer RG, Osterreicher CH, Takahashi H, Karin M. Dietary and genetic obesity promote liver inflammation and tumorigenesis by enhancing IL-6 and TNF expression. *Cell* 2010;140:197–208.
23. Nelson JE, Handa P, Aouizerat B, Wilson L, Vemulakonda LA, Yeh MM, Kowdley KV, Network NCR. Increased parenchymal damage and steatohepatitis in Caucasian non-alcoholic fatty liver disease patients with common IL1B and IL6 polymorphisms. *Aliment Pharmacol Ther* 2016;44:1253–1264.
24. Luo XY, Takahara T, Kawai K, Fujino M, Sugiyama T, Tsuneyama K, Tsukada K, Nakae S, Zhong L, Li XK. IFN-gamma deficiency attenuates hepatic inflammation and fibrosis in a steatohepatitis model induced by a methionine- and choline-deficient high-fat diet. *Am J Physiol Gastrointest Liver Physiol* 2013;305:G891–G899.
25. Kobayashi M, Fitz L, Ryan M, Hewick RM, Clark SC, Chan S, Loudon R, Sherman F, Perussia B, Trinchieri G. Identification and purification of natural killer cell stimulatory factor (NKSF), a cytokine with multiple biologic effects on human lymphocytes. *J Exp Med* 1989;170:827–845.
26. Kiu H, Nicholson SE. Biology and significance of the JAK/STAT signalling pathways. *Growth Factors* 2012;30:88–106.
27. O’Shea JJ, Gadina M, Schreiber RD. Cytokine signaling in 2002: new surprises in the Jak/Stat pathway. *Cell* 2002;109(Suppl):S121–S131.
28. Chen W, Zhang J, Fan HN, Zhu JS. Function and therapeutic advances of chemokine and its receptor in nonalcoholic fatty liver disease. *Therap Adv Gastroenterol* 2018;11:1756284818815184.
29. Marra F, Tacke F. Roles for chemokines in liver disease. *Gastroenterology* 2014;147:577–594 e1.
30. Mohs A, Kuttkat N, Reissing J, Zimmermann HW, Sonntag R, Proudfoot A, Youssef SA, de Bruin A, Cubero FJ, Trautwein C. Functional role of CCL5/RANTES for HCC progression during chronic liver disease. *J Hepatol* 2017;66:743–753.
31. Hamilton JA. GM-CSF in inflammation. *J Exp Med* 2020:217.
32. Pillarisetty VG, Miller G, Shah AB, DeMatteo RP. GM-CSF expands dendritic cells and their progenitors in mouse liver. *Hepatology* 2003;37:641–652.
33. Leung TM, Nieto N. CYP2E1 and oxidant stress in alcoholic and non-alcoholic fatty liver disease. *J Hepatol* 2013;58:395–398.
34. Aaronson DS, Horvath CM. A road map for those who don’t know JAK-STAT. *Science* 2002;296:1653–1655.
35. Jung KH, Yoo W, Stevenson HL, Deshpande D, Shen H, Gagea M, Yoo SY, Wang J, Eckols TK, Bharadwaj U, Tweardy DJ, Beretta L. Multifunctional effects of a small-molecule STAT3 inhibitor on NASH and hepatocellular carcinoma in mice. *Clin Cancer Res* 2017;23:5537–5546.
36. Gao B, Wang H, Lafdil F, Feng D. STAT proteins: key regulators of anti-viral responses, inflammation, and tumorigenesis in the liver. *J Hepatol* 2012;57:430–441.

37. Tron K, Samoilenko A, Musikowski G, Kobe F, Immenschuh S, Schaper F, Ramadori G, Kietzmann T. Regulation of rat heme oxygenase-1 expression by interleukin-6 via the Jak/STAT pathway in hepatocytes. *J Hepatol* 2006;45:72–80.
38. Dela Pena A, Leclercq I, Field J, George J, Jones B, Farrell G. NF-kappa B activation, rather than TNF, mediates hepatic inflammation in a murine dietary model of steatohepatitis. *Gastroenterology* 2005;129:1663–1674.
39. Mertens C, Darnell JE Jr. SnapShot: JAK-STAT signaling. *Cell* 2007;131:612.
40. Charni-Natan M, Goldstein I. Protocol for primary mouse hepatocyte isolation. *STAR Protoc* 2020;1:100086.

CRediT Authorship Contributions

Feixue Wang (Conceptualization: Equal; Data curation: Lead; Formal analysis: Lead; Investigation: Lead; Methodology: Lead; Writing – original draft: Lead)

Xiang Zhang (Conceptualization: Supporting; Supervision: Supporting; Writing – review & editing: Supporting)

Weixin Liu (Formal analysis: Supporting; Methodology: Supporting)

Yunfei Zhou (Investigation: Supporting; Methodology: Supporting)

Wenchao Wei (Investigation: Supporting; Methodology: Supporting)

Dabin Liu (Investigation: Supporting; Methodology: Supporting)

Chi-Chun Wong (Investigation: Supporting; Writing – review & editing: Supporting)

Joseph J. Y. Sung (Conceptualization: Supporting; Resources: Supporting)

Jun Yu, MD, PhD (Conceptualization: Lead; Funding acquisition: Lead; Supervision: Lead; Writing – review & editing: Lead)

Conflicts of interest

The authors disclose no conflicts.

Received May 3, 2021. Accepted August 23, 2021.

Correspondence

Address correspondence to: Jun Yu, MD, PhD, Department of Medicine and Therapeutics, The Chinese University of Hong Kong, Hong Kong SAR, China. e-mail: junyu@cuhk.edu.hk; fax: (852) 21445330.

Funding

Supported by RGC Theme-based Research Scheme Hong Kong (T12-703/19-R), RGC Collaborative Research Fund (C4041-17GF, C7026-18GF), HMRF Hong Kong (07181256), and Vice-Chancellor's Discretionary Fund CUHK.